

Dynamic Ultraslow Optical-Matter Wave Analog of an Event Horizon

C. J. Zhu,^{1,2} L. Deng,¹ E. W. Hagley,¹ and Mo-Lin Ge³

¹*National Institute of Standards & Technology, Gaithersburg, Maryland 20899, USA*

²*School of Physics Science and Engineering, Tongji University, Shanghai 200092, China*

³*Theoretical Physics Division, Chern Institute of Mathematics, NanKai University, Tianjin 300071, People's Republic of China*

(Received 16 April 2014; published 28 August 2014)

We investigate theoretically the effects of a dynamically increasing medium index on optical-wave propagation in a rubidium condensate. A long pulsed pump laser coupling a $D2$ line transition produces a rapidly growing internally generated field. This results in a significant optical self-focusing effect and creates a dynamically growing medium index anomaly that propagates ultraslowly with the internally generated field. When a fast probe pulse injected after a delay catches up with the dynamically increasing index anomaly, it is forced to slow down and is prohibited from crossing the anomaly, thereby realizing an ultraslow optical-matter wave analog of a dynamic white-hole event horizon.

DOI: [10.1103/PhysRevLett.113.090405](https://doi.org/10.1103/PhysRevLett.113.090405)

PACS numbers: 03.75.-b, 42.50.Gy, 42.65.-k, 52.72.+v

Cosmic phenomena are some of the most fascinating aspects of science that have been imagined and studied ever since the dawn of civilization. While such phenomena occur on astronomical scales deep in the Universe under extreme conditions, there have been efforts to study these fascinating events on Earth by means of analog models that can be realized in various physical systems. Unruh [1,2] first proposed the possibility of reproducing the space-time geometry of a black hole by studying sound waves in a flowing medium. In the past decade, many analog studies associated with this and other cosmic phenomena have been reported. These include the study of an event horizon surrounding a black hole and a white hole in fluids [3,4], the study of Hawking radiation in superfluid helium [5,6], and studies based on ultrashort pulse filamentation in solids [7,8]. Several physical systems for observing white-hole event horizons [9,10] and Hawking radiation [11] in photonic crystal fibers and Bose-Einstein condensates (BECs) [12,13] have also been proposed. Experimentally, a matter-wave analog of a supernova [14] and a sonic analog of a black hole event horizon [15] have been explored in BECs.

Surprisingly, atoms are among the most powerful physical systems that can be used to investigate cosmic phenomena. The interaction between photons and atoms has been intensively and broadly investigated theoretically and experimentally since the dawn of quantum mechanics and is arguably the best approach to mimic cosmic phenomena in a ground-based laboratory, as shown in recent studies using BECs [12–14]. Indeed, the theoretical simplicity and the relative ease with which BECs can be controlled under laboratory conditions have made BECs a much sought after laboratory-based system for investigation of astrophysical phenomena.

Recently, an interesting analog of a cosmic phenomenon was demonstrated using a specially engineered photonic

optical fiber with high power femtosecond lasers [9,10]. In this study, a femtosecond laser pulse with an enormous peak intensity traveled along the fiber, creating a large but highly localized traveling index anomaly arising from the intensity-dependent Kerr effect. A fast, short probe pulse delay injected after this transient-index-deformation laser pulse sees a strong positive index gradient, and therefore encounters a significant group velocity change since $V_g = c/(n + \omega(\partial n/\partial \omega))$. In consequence, it can never reach a high enough velocity to surpass the index anomaly, and this is an analog of a white-hole event horizon.

In this Letter, we describe an ultraslow optical-wave analog of an astrophysical event horizon in a Bose-Einstein condensate using a coherent light-matter-wave mixing technique. Here, we focus on the event horizon effect arising from light-matter wave mixing and coherent propagation. The motivation arises from the fact that in an optical-matter wave-mixing process under red-detuned excitation with pulse durations exceeding $100 \mu\text{s}$ the rapid growth of an ultraslowly propagating mixing-wave field in a high-density condensate results in a highly localized transverse optical field distribution. Consequently, there is a significant optical-dipole force that compresses the atomic density distribution, resulting in a significant traveling index anomaly that grows rapidly. When a weak probe field traveling in the same direction as the mixing wave but with a faster group velocity is injected into the medium after a delay, it catches up with the rapidly growing but ultraslowly propagating index anomaly. The index anomaly behaves as a barrier forcing the fast probe field to slow down and to stay on the tail of the index anomaly. In essence, the probe light is forced to “surf” the ultraslow and ultracold index wave.

There are a number of fundamental differences between this optical-matter wave analog and the index anomaly induced by a high-energy femtosecond pulse in a photonic

fiber. Contrary to the static process in the photonic-fiber scheme [9,10], the light-matter wave system is highly dynamic because the barrier height increases continuously and rapidly due to the amplification of the mixing wave as it propagates in the medium [16]. In the case of a solid medium, atoms cannot leave their lattice sites and in the frame that is moving with the high energy pulse both the index change and the event horizon are static. Consequently, there is no positive growth feedback resulting from actual atom motion by dipole-force compression, as there is in our case. In the optical-matter wave scheme the motion of atoms caused by optical compression leads to a real density change that is seen by the ultraslowly propagating mixing wave. This causes the slope of the index anomaly to increase continuously in the moving frame [17], resulting in a dynamic event horizon [18] growing faster than the laser pulse profile. These dynamic features are intrinsically lacking in the static photonic-fiber systems studied in Refs. [9,10]. To demonstrate these features we show by numerical calculation that a delay-injected probe field is forced by the ultraslow index anomaly (i.e., the event horizon) to slow down. It is also partially reflected as it reaches the positive slope of the index anomaly, resulting in an interference between the incident field and the probe field reflected by the white event horizon, an intriguing signature of the process.

We consider a cylindrically shaped ^{87}Rb condensate of length L (Fig. 1) with a uniform density distribution along its z axis. The condensate's initial transverse density profile is given by $n(\rho) = n_0(1 - \rho^2/\rho_0^2)$, where n_0 is the peak density. Here, $\rho = \sqrt{x^2 + y^2}$ is the radial coordinate and ρ_0 is the initial transverse radius of the condensate. The condensate is excited along its long axis by a uniform pulsed pump field $\mathbf{E}_L(\omega_L)$, which is polarized in the x direction and travels in the $+z$ direction. The pump field typically has a pulse length $\tau_p \approx 300 \mu\text{s}$ and it drives the

$|5S_{1/2}, F=1\rangle \leftrightarrow |5P_{3/2}, F=1\rangle$ transition with a large one-photon detuning δ_L to avoid spontaneous emission. In this excitation geometry, only the field $E_G(\rho, z, t)$ with angular frequency ω_G propagating in the $-z$ direction can be generated with an appreciable gain due to the suppression of small angle collinear scattering by the condensate's structure factor [19].

In the slowly varying envelope approximation, the Maxwell equation for the generated field is given by

$$\begin{aligned} -i \frac{\partial \epsilon^{(+)}}{\partial z} + \frac{i}{c} \frac{\partial \epsilon^{(+)}}{\partial t} + \frac{1}{2k_G} \nabla_{\perp}^2 \epsilon^{(+)} \\ = \frac{\kappa_0 |\psi_0|^2}{\delta_L + i\Gamma} \epsilon^{(+)} + \frac{\kappa_0}{\delta_L + i\Gamma} \sum_n \psi_n \psi_{n+1}^* e^{i2(n+1)4\omega_R t - i\delta_L t}, \end{aligned} \quad (1)$$

where the polarization source term is expressed using the multiorder Fourier-decomposed Gross-Pitaevskii (G-P) equation [20]. In Eq. (1), $k_G = 2\pi/\lambda_G$ where λ_G is the wavelength of the generation field, $\kappa_0 = 2\pi|D_{12}|^2/c\hbar$ with D_{12} being the dipole matrix element. $|\psi_0|^2 \approx N_0$ is the average atom density, and $\omega_R = 2\hbar^2 k_L^2/M$ is the first-order recoil frequency with k_L and M being the pump-laser wave vector and the mass of the atom, respectively. In addition, δ_L and Γ are the one-photon laser detuning to the upper electronic excited state and the spontaneous emission rate of this state. The normalized wave-mixing field is defined as $\epsilon^{(\pm)} = E_G^{(\pm)}(\rho, z, t)/E_L^{(\pm)}$.

The n th order mean-field atomic wave function satisfies

$$\begin{aligned} \frac{\partial \psi_n}{\partial t} = & -\gamma_n \psi_n - i \nabla_{\perp}^2 \psi_n - i g_0 \delta_L |\epsilon^{(+)}|^2 \psi_n \\ & - i g \sum_{m_1, m_2} \psi_{m_1} \psi_{m_2}^* \psi_{n-m_1+m_2} S_{n, m_1, m_2} \\ & - i g_0 \delta_L \sum_{\pm} \epsilon^{(\pm)} \psi_{n\pm 1} e^{-i(\omega_{n\pm 1} - \omega_n) t \pm i\delta_L t}. \end{aligned} \quad (2)$$

Here, $S_{n, m_1, m_2} = e^{i(\omega_n - \omega_{m_1} + \omega_{m_2} - \omega_{n-m_1+m_2}) t}$, $g = 4\pi\hbar^2 a/M$ with a being the scattering length and $g_0 \approx |D_{12}|^2 |E_L|^2 / \hbar^2 \delta_L^2$. In addition, $\hbar\omega_m = 2(m\hbar k_L)^2/M$ is the m th order recoil energy and we have enforced photon-atom momentum conservation (i.e., $\mathbf{K} = \mathbf{k}_L - \mathbf{k}_G$ where \mathbf{K} is the recoil momentum). The γ_n term characterizing the loss of coherence of the n th order atomic center-of-motion wave function has been added phenomenologically and in the case of first-order scattering this momentum state relaxation rate has been measured [21]. We emphasize that it is crucial to include the optical-dipole potential due to the generated field because it grows rapidly in the condensate [22].

To investigate the fast growing index anomaly associated with the rapid growth of the mixing-wave field, Eqs. (1) and (2) must be solved simultaneously. To this end, we numerically integrate Eqs. (1) and (2) with $n = 0, 1$ [23]. In Fig. 1, we show the condensate cross-section change

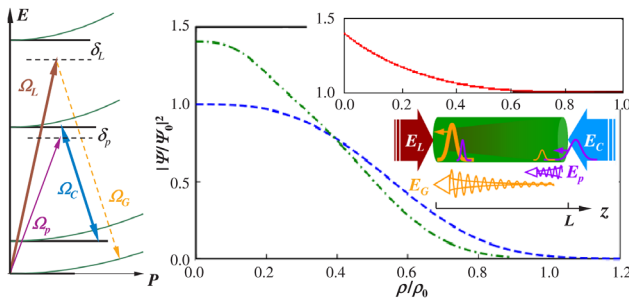


FIG. 1 (color online). Left: energy level diagram with laser couplings. Right: density distribution as a function of ρ/ρ_0 at the condensate entrance ($z/L = 1$, dashed curve), and exit ($z/L = 0$, dash-dotted curve). Inset plot: matter-wave index anomaly along the long axis ($\rho = 0$) as a function of z/L . The backward-propagating mixing wave starts at $z/L = 1.0$ where the index anomaly is negligible. The index anomaly reaches maximum at $z/L = 0$ after a full length of travel with gain.

resulting from the high gain mixing-wave process. In the inset in the upper right corner the matter-wave index anomaly is plotted as a function of the normalized propagation distance z/L . Near its end of travel, the mixing wave is maximal and the index anomaly peaks. This is where the most significant condensate transverse compression, and therefore index anomaly, occurs. The substantial change in density and in the optical index as the growing mixing wave propagates through the condensate provides the conceptual foundation for an ultraslow and ultracold optical-matter wave white event horizon with a delay-injected probe field (see below).

Our objective is to study the behavior of an optical probe field as it approaches the dynamically increasing index anomaly moving in space and time. This requires a detailed understanding of the index anomaly, which, unfortunately, cannot be easily extracted from direct numerical integration of Eqs. (1) and (2). In the following, we attempt to establish the validity of an analytical theory based on a third-order perturbation treatment of the light-matter, wave-mixing process. The analytic results can, if sufficiently accurate, be directly used to investigate the moving index anomaly and the effect of an event horizon on the delay-injected probe field.

In third-order perturbation theory we insert

$$\psi_0 = \psi_0^{(0)} + \lambda^2 \psi_0^{(2)}, \quad \psi_1 = \lambda \psi_1^{(1)} + \lambda^3 \psi_1^{(3)}, \quad (3)$$

into Eq. (2) and enforce the first-order Bragg scattering condition $\omega_1 - \omega_0 = 4\omega_R = \delta_L$. Keeping all terms up to third order in the wave-mixing field (as usual, $\epsilon^{(+)}$ is treated as the first-order small quantity) we obtain corrections to the atomic mean-field wave functions

$$\psi_0^{(2)} = -i\delta_L g_0 \psi_0^{(0)} A |\epsilon^{(+)}|^2, \quad (4a)$$

$$\psi_{+1}^{(1)} = -i \frac{\delta_L g_0 \psi_0^{(0)}}{\gamma_1 + ig|\psi_0^{(0)}|^2} \epsilon^{(-)}, \quad (4b)$$

$$\psi_{+1}^{(3)} = -\frac{\delta_L^2 g_0^2 \psi_0^{(0)}}{\gamma_1 + ig|\psi_0^{(0)}|^2} B |\epsilon^{(+)}|^2 \epsilon^{(-)}, \quad (4c)$$

where A and B are given in Ref. [24] and $|\psi_0^{(0)}|^2 = \mathcal{N}_0$ with $\psi_0^{(0)}$ being obtained by solving the stationary G-P equation in the absence of the external electric field numerically [i.e., the solution of Eq. (2) without $\epsilon^{(\pm)}$].

Substituting Eqs. (4a)–(4c) into Eq. (1) leads to a third-order wave equation analog of a (2+1)D nonlinear Schrödinger equation [25,26],

$$i \frac{\partial \epsilon^{(+)}}{\partial z} - i \frac{1}{V_g^{(G)}} \frac{\partial \epsilon^{(+)}}{\partial t} - \frac{1}{2k_G} \nabla_{\perp}^2 \epsilon^{(+)} = (W + \beta) \epsilon^{(+)}, \quad (5a)$$

$$W \approx \frac{\kappa_0 \delta_L g_0^2 \mathcal{N}_0}{\gamma_1} \left(\frac{5\delta_L g_0 \mathcal{N}_0}{\gamma_1} - 3 - 2i \frac{\delta_L}{\gamma_1} \right) |\epsilon^{(+)}|^2, \quad (5b)$$

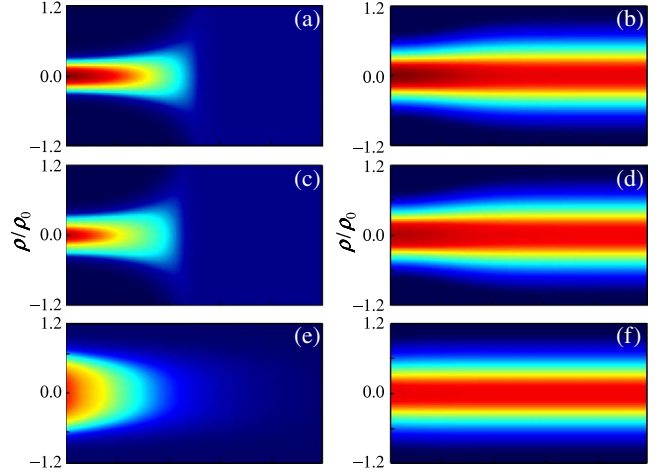


FIG. 2 (color online). Mixing wave intensity (a),(c),(e) and condensate density distribution (b),(d),(f) as a function of z/L (horizontal axis) and ρ/ρ_0 with and without nonlinear term $|\epsilon^{(+)}|^2$. (a),(b) Numerical solutions of Eqs. (1) and (2). (c),(d) Results from Eqs. (4) and (5). (e),(f) Numerical solution of Eqs. (1) and (2) without the nonlinear term $|\epsilon^{(+)}|^2$. $|\psi_0|^2 \approx 4.0 \times 10^{12} \text{ cm}^{-3}$, $\Gamma/2\pi = 6 \text{ MHz}$, $\gamma_1/2\pi = 2 \text{ kHz}$, $\tau_P = 300 \mu\text{s}$, $\kappa_0 = 2.76 \times 10^{-6} \text{ m}^2 \text{ s}^{-1}$, $g/\hbar = 4.85 \times 10^{-17} \text{ m}^3 \text{ s}^{-1}$, $\delta_L/2\pi = -2 \text{ GHz}$, $k_G \approx 8 \times 10^6 \text{ m}^{-1}$, $g_0 = 1.3 \times 10^{-5}$.

where $\beta = -i\kappa_0 g_0 \mathcal{N}_0 / \gamma_1$ leads to a propagation gain. The mixing wave starts at $z = L$ and propagates toward $z = 0$ with an ultraslow group velocity given by $1/V_g^{(G)} = 1/c + \kappa_0 g_0 \mathcal{N}_0 / \gamma_1^2$. Figures 2(c) and 2(d) depict the numerical evaluation of Eqs. (4) and (5) and show clearly that the approximated analytic solutions capture the main physics of the coherent optical-matter wave-mixing process [compare with Figs. 2(a) and 2(b), which are obtained by direct integration of Eqs. (1) and (2)]. This crucial verification, which shows both the importance of the nonlinear term and the validity of the analytical solutions given in Eqs. (4) and (5), provides the foundation that will be used to investigate the formation of an event horizon.

Next, we discuss the effect of the index anomaly that causes the white event horizon. As the index anomaly produced by the wave-mixing process propagates ultraslowly along the long axis of the condensate, a weak probe field E_P (coupling the $|5S_{1/2}, F=1\rangle \leftrightarrow |5P_{1/2}, F=2\rangle$ transition) and a strong control field E_C (coupling the $|5P_{1/2}, F=2\rangle \leftrightarrow |5S_{1/2}, F=2\rangle$ transition) are injected. These two additional fields propagate along the mixing-wave propagation direction (i.e., the $-z$ direction) with a slight time delay, forming an electromagnetically induced transparency (EIT) configuration. The time delay and the large separation between the $D1$ line (for EIT ultraslow probe propagation) and the $D2$ line (for wave mixing and index anomaly generation) ensure there is no cross talk between the index anomaly (wave mixing) producing process and the EIT ultraslow probe-field propagation process. We adjust the

control field E_C to make the probe field group velocity $V_g^{(p)}$ larger than that of the index anomaly, i.e., the group velocity $V_g^{(G)}$ of the generated mixing wave.

In Fourier space, the linear susceptibility of the probe field is given by $\chi_p(\omega; z) = \chi_p(z)W(\omega)$, where $\chi_p(z) = |D|^2 \mathcal{N}_a(z)/(2\epsilon_0 \hbar)$ and [27]

$$W(\omega) = \frac{(\omega + \delta_{2\text{ph}} + i\gamma_2)}{|\Omega_C|^2 - (\omega + \delta_{2\text{ph}} + i\gamma_2)(\omega + \delta_p + i\Gamma)}. \quad (6)$$

Here δ_p is the probe detuning and $|D|$ is the matrix element for the transition coupled by the probe field. In the case of EIT, the two-photon detuning $\delta_{2\text{ph}} = \delta_p - \delta_C = 0$, where δ_C is the coupling-field detuning.

In Eq. (6), the propagation-dependent index is $\mathcal{N}_a(z) = 1/V_0 \int_0^{\sigma_p} |\psi(\rho, z)|^2 d\rho/\sigma_p$, where $\sigma_p \leq \rho_0$ is the transverse radius of the probe field ($V_0 = \pi\rho_0^2 L$). This results in a propagation-dependent group velocity $V_g^{(p)}(\omega; z) = c/\{n_L(\omega; z) + \omega_p[\partial n_L(\omega; z)/\partial \omega_p]\}$, where the dynamic local index of refraction of the medium becomes $n_L(\omega; z) = \sqrt{1 + \chi_p(\omega; z)} = n'(\omega; z) + in''(\omega; z)$. As the probe field catches up with the moving index anomaly, its group velocity is continuously reduced by the increasing local index anomaly. In essence, the wave front of the probe field is blocked by the wave-mixing field and prohibited from crossing the index anomaly, which is an analog of a white event horizon for the probe field.

In Figs. 3(a) and 3(b), we show the probe group velocity $V_g^{(p)}$ as a function of δ_p and ρ/ρ_0 at the probe entrance $z = L$ and exit $z = 0$. At the probe entrance $z = L$, we find $V_g^{(p)} > V_g^{(G)}$. In fact, it is easy to show analytically using Eqs. (4) and (5) that $V_g^{(G)} \approx 1.0$ m/s. Therefore, the delay-injected probe field chases the mixing wave along the long axis of the condensate. As the mixing-wave intensity builds up, the probe experiences an increasing index anomaly as it approaches the mixing wave. The increasing mixing wave produces a dynamically increasing “index barrier” that prevents the faster probe from crossing it by reducing its group velocity. This feature is further exhibited in Fig. 3(c) where the probe group velocity is plotted along the condensate’s long axis ($\rho = 0$). This plot shows a region of δ_p in which $V_g^{(p)} \leq V_g^{(G)}$ is forced on the probe field and a white event horizon for the probe field is realized.

The forced slow down of the probe near the event horizon can be vividly depicted by examining the interaction between the moving index anomaly and the delay-injected probe when the latter catches up with the index anomaly produced by the mixing wave. Intuitively, as the front edge of the probe approaches the dynamically increasing “barrier” (index anomaly), probe wave slow down, reflection, and subsequent self-interference with the remaining part of the still-approaching probe pulse will

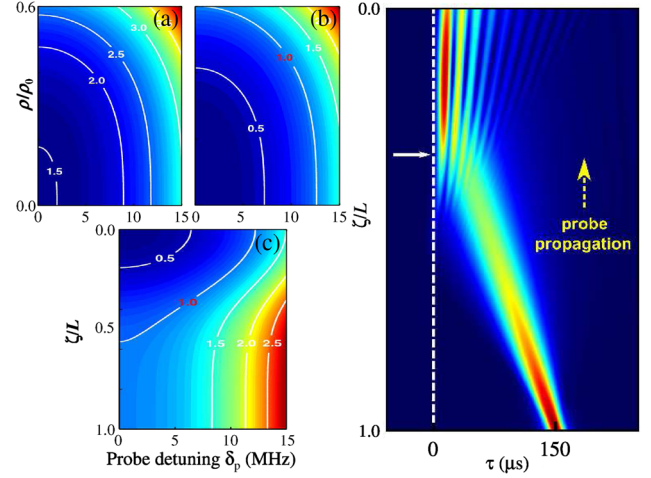


FIG. 3 (color online). Left panel: probe group velocity $V_g^{(p)}$, indicated by equal altitude lines, as a function of δ_p and ρ/ρ_0 at (a) entrance ($z/L = 1$) and (b) exit ($z/L = 0$). Mixing-wave velocity $V_g^{(G)} \approx 1.0$ m/s is indicated by the red number. (c) $V_g^{(p)}$ as a function of z/L and δ_p along the condensate’s long axis ($\rho = 0$). Right panel: evolution of the probe field as a function of z/L and τ in the mixing-wave co-moving reference. The dashed vertical line indicates the white event horizon in the moving frame. The solid arrow near the dashed line indicates where the faster probe catches the index anomaly and is subsequently slowed down and reflected.

occur. To verify this intuition we numerically integrate the Maxwell equation of the probe field E_p [28]

$$i \frac{2n^2}{c} \frac{\partial E_p}{\partial t} + \frac{1}{k_p} \frac{\partial^2 E_p}{\partial z^2} + k_p n(z)^2 E_p = 0. \quad (7)$$

Here, $E_p = \mathcal{A}_p(z; t)e^{-(t-\tau_D)^2/\tau_p^2}$ and $E_G = \mathcal{A}_G(z; t)e^{-t^2/\tau_G^2}$, where τ_G and τ_p are the pulse lengths of the generated and probe field, respectively. The probe delay is $\tau_D = 25 \mu\text{s}$ and the propagation-dependent index is obtained by solving the G-P equation.

In the right panel of Fig. 3 we graphically depict the propagation dynamics of the probe field in the reference frame moving with the mixing-wave E_G . The fast probe field with $V_g^{(p)} > V_g^{(G)}$ enters the medium about $150 \mu\text{s}$ after the mixing wave is generated at $z/L = 1$. It catches up with the trailing edge of the moving index anomaly created by the generated field, and is forced to reduce its propagation velocity. Finally, the index barrier reflects the front edge of the probe field, causing it to interfere with the rest of the probe field that is still approaching the index anomaly. This contour plot vividly exhibits the dynamic features of coherent wave-propagation effects on this analogous white-hole event horizon phenomenon.

The Hawking temperature [29–32] in our case can be estimated as in Refs. [8,9]. A 20% index increase and an optical pulse with a $1\text{-}\mu\text{s}$ rising edge results in a Hawking temperature of a few microKelvins. We note, however, that

the fast growing mixing wave, and therefore the index anomaly, makes the rising edge of the internally generated field much steeper than that of a typical Gaussian pulse. The combination of an optical field with a fast rising edge and a high density condensate would result in the generation of a wave-mixing field with very steep edges [33]. Estimates indicate that this would correspond to a 1-mK or higher Hawking temperature, which would generate a signal in the 50 MHz range and could, in principle, be detected using radio-frequency heterodyning techniques. We emphasize, however, that as the mixing wave grows in the medium the Hawking temperature increases since the front of the horizon becomes steeper and steeper. It is precisely the density distribution of the quantum gas and the mobility of the atoms under the influence of the significant dipole force created by the internally generated field that lead to this dynamic feature that does not exist in the case of soliton propagation in fibers.

In conclusion, we studied an optical-matter wave analog of a white event horizon using a Bose-Einstein condensate and a nonlinear wave-mixing process. The rapidly growing mixing wave leads to strong local-field effects, resulting in a significant local index anomaly that travels with the generated wave. This index anomaly impacts the group velocity of a weak probe field traveling in the same medium. In the frame of reference co-moving with the growing wave-mixing field, the index anomaly is temporally stationary, but the peak and the slope of the anomaly continuously increase in time, resulting in a dynamically increasing matter-wave barrier that prevents a probe field from crossing the event horizon.

We thank Professors Q. Y. Cai and B. C. Zhang for discussions.

-
- [1] W. G. Unruh, *Phys. Rev. D* **51**, 2827 (1995).
 [2] M. Visser, *Classical Quantum Gravity* **15**, 1767 (1998).
 [3] L. Susskind, *Sci. Am.*, **276**, No 4, 52 (1997).
 [4] A. Cho, *Science* **319**, 1321 (2008).
 [5] T. A. Jacobson, *Phys. Rev. D* **44**, 1731 (1991).
 [6] T. A. Jacobson and G. E. Volovik, *Phys. Rev. D* **58**, 064021 (1998).
 [7] F. Belgiorno, S. L. Cacciatori, M. Clerici, V. Gorini, G. Ortenzi, L. Rizzi, E. Rubino, V. G. Sala, and D. Faccio, *Phys. Rev. Lett.* **105**, 203901 (2010).
 [8] R. Schützhold and W. G. Unruh, *Phys. Rev. Lett.* **107**, 149401 (2011).
 [9] T. G. Philbin, C. Kuklewicz, S. Robertson, S. Hill, F. König, and U. Leonhardt, *Science* **319**, 1367 (2008).
 [10] A. Demircan, Sh. Amiranashvili, and G. Steinmeyer, *Phys. Rev. Lett.* **106**, 163901 (2011).
 [11] D. Faccio, *Contemp. Phys.* **53**, 97 (2012).
 [12] L. J. Garay, J. R. Anglin, J. I. Cirac, and P. Zoller, *Phys. Rev. Lett.* **85**, 4643 (2000).
 [13] L. J. Garay, J. R. Anglin, J. I. Cirac, and P. Zoller, *Phys. Rev. A* **63**, 023611 (2001).
 [14] E. A. Donley, N. R. Claussen, S. L. Cornish, J. L. Roberts, E. A. Cornell, and C. E. Wieman, *Nature (London)* **412**, 295 (2001).
 [15] O. Lahav, A. Itah, A. Blumkin, C. Gordon, S. Rinott, A. Zayats, and J. Steinhauer, *Phys. Rev. Lett.* **105**, 240401 (2010).
 [16] Y. R. Shen, *The Principles of Nonlinear Optics* (John Wiley & Sons, New York, 1984).
 [17] L. Deng, M. G. Payne, and E. W. Hagley, *Phys. Rev. Lett.* **104**, 050402 (2010).
 [18] This dynamic growth of the event horizon may have some similarities with the expansion of the event horizon of a black hole consuming the mass of a nearby star.
 [19] L. Deng, C. J. Zhu, and E. W. Hagley, *Phys. Rev. Lett.* **110**, 210401 (2013). The mixing-wave gain is $G_q \propto S(q)$, where $S(q \rightarrow 0) \rightarrow 0$ (forward) and $S(q \gg 0) \rightarrow 1$ (backward).
 [20] M. G. Moore and P. Meystre, *Phys. Rev. Lett.* **83**, 5202 (1999).
 [21] J. Stenger, S. Inouye, A. Chikkatur, D. Stamper-Kurn, D. Pritchard, and W. Ketterle, *Phys. Rev. Lett.* **82**, 4569 (1999). The γ_n are chosen to ensure total population conservation.
 [22] Since the initial and final states in this light-matter wave-mixing scheme are the same electronic ground state, the pump-induced Stark shift does not contribute to Eq. (1).
 [23] For long pulses, $n < 0$ orders are not important. In addition, adding $n > 1$ terms does not affect the fundamental conclusion of this study. See, L. Deng and E. W. Hagley, *Phys. Rev. A* **82**, 053613 (2010).
 [24] C. J. Zhu, L. Deng, E. W. Hagley, and G. X. Huang, *Laser Phys.* **24**, 065402 (2014).
 [25] We neglected the $(1/c)(\partial\epsilon/\partial t)$ term because of the dominant ultraslow propagation velocity. See Ref. [20] and M. G. Payne and L. Deng, *Phys. Rev. A* **64**, 031802(R) (2001).
 [26] Taking $\gamma_1 \gg g|\psi_0^{(0)}|^2$ and $|\delta_L| \gg \Gamma$. See Ref. [24].
 [27] C. J. Zhu, C. Hang, and G. X. Huang, *Eur. Phys. J. D* **56**, 231 (2010).
 [28] C. J. Zhu and G. X. Huang, *Opt. Express* **19**, 1963 (2011).
 [29] C. Barceló, S. Liberati, and M. Visser, *Int. J. Mod. Phys. A* **18**, 3735 (2003).
 [30] S. Giovanazzi, *Phys. Rev. Lett.* **94**, 061302 (2005).
 [31] L. J. Garay, J. R. Anglin, J. I. Cirac, and P. Zoller, *Phys. Rev. Lett.* **85**, 4643 (2000).
 [32] C. Mayoral, A. Recati, A. Fabbri, R. Parentani, R. Balbinot, and I. Carusotto, *New J. Phys.* **13**, 025007 (2011).
 [33] We note that higher order wave-mixing processes under high pump rate permit multiple scattering per atom, resulting in much higher local field intensity than the first order treatment shown here.